Egg-Sphingomyelin and Cholesterol Form a Stoichiometric Molecular Complex in Bilayers of Egg-Phosphatidylcholine

Peter J. Quinn*,†,‡ and Claude Wolf†,§

Department of Biochemistry, King's College London, 150 Stamford Street, London SE1 9NH, United Kingdom, and Universite Pierre et Marie Curie-Paris 6, Faculte de Medecine, Paris 75012, France

Received: August 9, 2010; Revised Manuscript Received: October 11, 2010

Sphingomyelin and cholesterol are membrane lipids that interact to form liquid-ordered phase believed to act as a platform for the organization of signaling proteins. We report analyses of synchrotron X-ray powder diffraction patterns recorded from aqueous dispersions of ternary mixtures of sphingomyelin and phosphatidylcholine from egg yolk and cholesterol to investigate how cholesterol distributes between the two phospholipids. In the absence of cholesterol the two phospholipids are immiscible between 20 and 50 °C. Addition of up to 22 mol % cholesterol to equimolar mixtures of the phospholipids results in partition of some sphingomyelin into a phosphatidylcholine phase at 37 °C. Increased proportions of cholesterol result in partition of the excess cholesterol into the phosphatidylcholine phase which is in equilibrium with a stoichiometric complex of 1.7:1, sphingomyelin:cholesterol. The molecular order of the complex may explain the basis upon which proteins are assembled within the membrane raft.

Introduction

Formation of lipid domain structures in biological membranes has excited considerable interest as a possible mechanism of control and modulation of a variety of physiological functions such as transmembrane signal transduction, membrane differentiation, fusion, etc.[1−4] The isolation of lipid domains from membranes and their characterization has proved problematic,[5] and model membranes composed of lipid mixtures dispersed in aqueous media have been extensively used to define the principles governing domain formation.[6,7] Codispersions of synthetic, molecularly defined lipids in aqueous media have been favored systems to model this behavior because they exhibit phase separations and domain structures that are amenable to study. Nevertheless, model systems of this type may oversimplify what in biological membranes is a highly complex assortment of widely differing molecular species of lipids.

Among the multitude of lipid molecular species that dominate the outer leaflet of the plasma membrane of eukaryotic cells most are associated with phosphatidylcholine and sphingomyelin. Molecular species of sphingomyelin, mostly defined by the amide-linked fatty acid, tend to have long, more saturated hydrocarbon substituents compared with phosphatidylcholines, where the fatty acyl residues are shorter and, particularly at the *sn*-2 position of the glycerol, more unsaturated. Cholesterol is another prominent component of the cell membrane. A preferential interaction of cholesterol with the longer chain, more saturated molecular species of lipid is well documented,[8] and this is said to be responsible for driving lipid phase separation to create coexisting liquid-ordered and liquid-disordered domains in bilayers.[9−13] Membrane proteins are also known to influence the distribution of cholesterol and to stabilize cholesterol-rich membrane domains.[14] Sphingomyelins of biological origin form gel-phase bilayers that undergo a gel to liquid-disordered phase transition at an onset temperature of about 35 °C and an end temperature of about 44 °C.[15] The phase properties of sphingomyelin are modified by the presence of cholesterol in a manner that depends on the proportion of cholesterol in the mixture.[16,17]

A phase formed with equimolar proportions of cholesterol and molecular species of sphingomyelin found in cell membranes has properties intermediate between gel (L_β) and liquid-disordered phase (L_d), a so-called, liquid-ordered phase (L_o).[18,19] Evidence for formation of L_o phase in mixtures of phosphatidylcholines and cholesterol is more problematic with earlier reports supporting such interactions at temperatures significantly greater than the gel to liquid-crystal transition of the phospholipid[20−22] being questioned by more recent studies.[23−26] These discrepancies could arise from investigations undertaken in time frames not matched with the L_o structure viewed as an assembly of metastable nanodomains in a condensed phase.

The present study was undertaken to determine the distribution of cholesterol between sphingomyelin and phosphatidylcholine from egg yolk. The characteristic feature of the molecular species of these two lipids is that they are both constituted with hydrocarbon chains predominantly of C16−18 in length. Previous studies have shown that binary mixtures of the two phospholipids are largely immiscible over the temperature range from 20 to 50 °C when the phosphatidylcholine is in the fluid phase and the sphingomyelin is in either the gel or the fluid phase.[27] The presence of small amounts of cholesterol results in partial miscibility of the two phospholipids. Increasing proportions of cholesterol result in phase separation of a structure comprised of a mixture of sphingomyelin and cholesterol coexisting with a phosphatidylcholine-rich structure. A composition phase diagram at 37 °C has been constructed from analysis of the X-ray data.

Materials and Methods

Lipids and Sample Preparation. Lipids were obtained and used without further purification as follows: egg-yolk L-α-

* To whom correspondence should be addressed. Phone: +44 2078484408. Fax: +44 2078484500. E-mail: p.quinn@kcl.ac.uk.
† Both authors contributed equally to the conception and performance of the experiments. P.J.Q. processed the results and wrote the paper.
‡ King's College London.
§ Universite Pierre et Marie Curie-Paris 6.

10.1021/jp107490a
Published on Web 11/04/2010

phosphatidylcholine (egg-PC, 770 Da), egg-yolk sphingomyelin (egg-SM, 703 Da), and cholesterol (387 Da) were purchased from Sigma (Sigma-Aldrich Chimie SARL, 38297 St. Quentin, France). Samples for X-ray diffraction examination were prepared by dissolving lipids in warm (45 °C) chloroform/methanol (2:1, vol/vol) and mixing them in the desired proportions (denoted as molar ratios in ternary mixtures). The organic solvent was subsequently evaporated under a stream of oxygen-free dry nitrogen at 45 °C, and any remaining traces of solvent were removed by storage under high vacuum for 2 days at 20 °C. The dry lipids were hydrated with an equal weight of water. This is sufficient to fully hydrate the lipids,[28] as demonstrated by the T_m of egg-SM in the mixture (35−40 °C). The methods used to disperse the lipids by mechanical and thermal cycling and conditions of storage prior to X-ray examination have been described elsewhere.[29] The dispersions were heated to 50 °C and cooled directly to 20 °C prior to recording the initial heating scan.

Synchrotron X-ray Diffraction Methods. X-ray diffraction measurements were performed on beamlines 2.1 of the Daresbury SRS and I22 of the Diamond SRS. The X-ray beam geometry was typically ∼0.2−0.5 mm focused on a mica sandwich cell with a surface of 2 × 5 mm. Simultaneous small-angle (SAXS) and wide-angle X-ray scattering (WAXS) intensities were recorded so that a correlation could be established between the mesophase repeat spacings and the packing arrangement of acyl chains. The SAXS intensity was recorded on 2-D RAPID detectors and the signal radially integrated to give a 1-D pattern. The WAXS intensity was recorded with 1-D HOTWAXS detectors. The sample to SAXS detector distance was 1.5 m, and calibration of d spacings was performed using silver behenate (d = 5.838 nm). The wide-angle X-ray scattering intensity profiles were calibrated using the diffraction peaks from high-density polyethylene.[30] The lipid dispersion (20 μL) was sandwiched between two thin mica windows 0.5 mm apart, and the measurement cell was mounted on a programmable temperature stage (Linkam, Surrey, U.K.). The temperature was monitored by a thermocouple inserted directly into the lipid dispersion (Quad Service, Poissy, France). The setup, calibration, and facilities available on the beamlines are described comprehensively on the respective Web sites: http://www.srs.dl.ac.uk/ncd/station21 and http://www.diamond.ac.uk/Home/Beamlines/I22.html. Data reduction and analysis were performed using OriginPro8 software (OriginLab Corp.).

Analysis of X-ray Diffraction Data. The small-angle X-ray scattering intensity profiles obtained from a sector integration of the 2-D powder pattern were analyzed using standard procedures.[31] Polarization and geometric corrections for line-width smearing were assessed by checking the symmetry of diffraction peaks in the present camera configuration using a sample of silver behenate. The orders of reflection could all be fitted by Gaussian + Lorentz symmetrical functions with fitting coefficients greater than $R^2 = 0.99$. Deconvolution is consistent with the sample to detector distance used.[32] After correction of the raw data by subtraction of the background scattering from both water and the sample cell, each of the Bragg peaks were fitted by a Lorentzian + Gaussian (Voigt) distribution by peak fitting performed using PeakFit 4.12 (Systat Software Inc.). This fit was compared with the fit of two or more Voigt functions to the peaks, and the best fit to the data with the fewest peaks was used. The method used for peak fitting has been described previously.[17] The analysis assumes that because the d spacings of the coexisting lamellar structures only differ by about 0.2 nm, scattering intensity is proportional to the lipid mass in the respective structures. An estimate of this error from the continuous Fourier transform of the electron density profile and examples of the peak fits to a second-order Bragg reflection are shown in Supporting Information Figure 1C. It should be noted that no information can be derived from lamellar Bragg reflections about the size of the domains in which the diffracting unit cells are comprised, but the order of the diffracting units is signified by the width of the peaks.

Results

To investigate the distribution of cholesterol in bilayers comprised of mixtures of egg-PC and egg-SM we first performed control experiments to characterize the miscibility of the two phospholipids in the absence of cholesterol. The thermotropic structural changes in aqueous dispersions of binary mixtures of the two phospholipids were examined by synchrotron X-ray diffraction methods during heating and cooling scans over the temperature range from 20 to 50 °C. This range spans the gel to fluid-phase transition of egg-SM. The scattering intensity profiles of the second-order lamellar reflections obtained from a binary mixture consisting of equimolar proportions of egg-PC and egg-SM is presented in Figure 1A. Peak assignments in this mixture have been made on the basis of d spacings (Figure 1B), scattering intensities (Figure 1C), and temperature-dependent changes in peak shape parameters (Figure 1D) (see Supporting Information). The results show that at least two coupled bilayer structures are present throughout the temperature range of the scan with an appearance of intermediate structures in the temperature range of the gel to fluid-phase transition of the egg-SM (35−39 °C). Thus, coexistence of two bilayer structures of egg-SM possibly comprised of bilayers with different molecular species one possibly forming an interdigitated bilayer[15,33] and fluid-phase egg-PC is observed at temperatures less than about 35 °C. At temperatures above 40 °C, judging from the wide-angle X-ray diffraction profile (Figure 1E), both lipids are in the fluid phase. Egg-SM forms a single bilayer structure in the fluid phase, and two bilayer structures can be deconvolved assigned to fluid-phase egg-PC. The phase separation at lower temperatures is due to exclusion by zone refining processes of lipids with low phase transition temperatures from the gel phase formed by molecular species of egg-SM. Phase separation at temperatures higher than the transition temperature of the gel to the fluid state is likely to be due to intermolecular hydrogen bonds that are formed between sphingomyelin molecules (see Discussion). For these structures to be resolved from the powder diffraction patterns the bilayers must be coupled in that bilayers of pure egg-PC must be distinguished structurally from bilayers of pure egg-SM. If the bilayers were not coupled broad Bragg reflections would be observed from which individual lamellar structures could not be resolved.

The effect of adding increasing amounts of cholesterol to equimolar mixtures of egg-PC and egg-SM on the structures of the bilayers during heating scans from 20 to 50 °C was investigated next. Figure 2 shows the results obtained from a dispersion comprised of egg-PC:egg-SM:cholesterol in molar proportions 47.5:47.5:5. An overview of the SAXS/WAXS scattering intensity profiles recorded during the initial heating scan shows the presence of two lamellar structures throughout the scan (Figure 2A). There is a progressive decrease in lamellar d spacing of both structures during heating from 20 °C to the onset of the phase transition of the egg-SM-enriched structure (33 °C), whereupon the rate of decrease of d spacing of the egg-SM-enriched phase is lower (Figure 2B). This disparity in

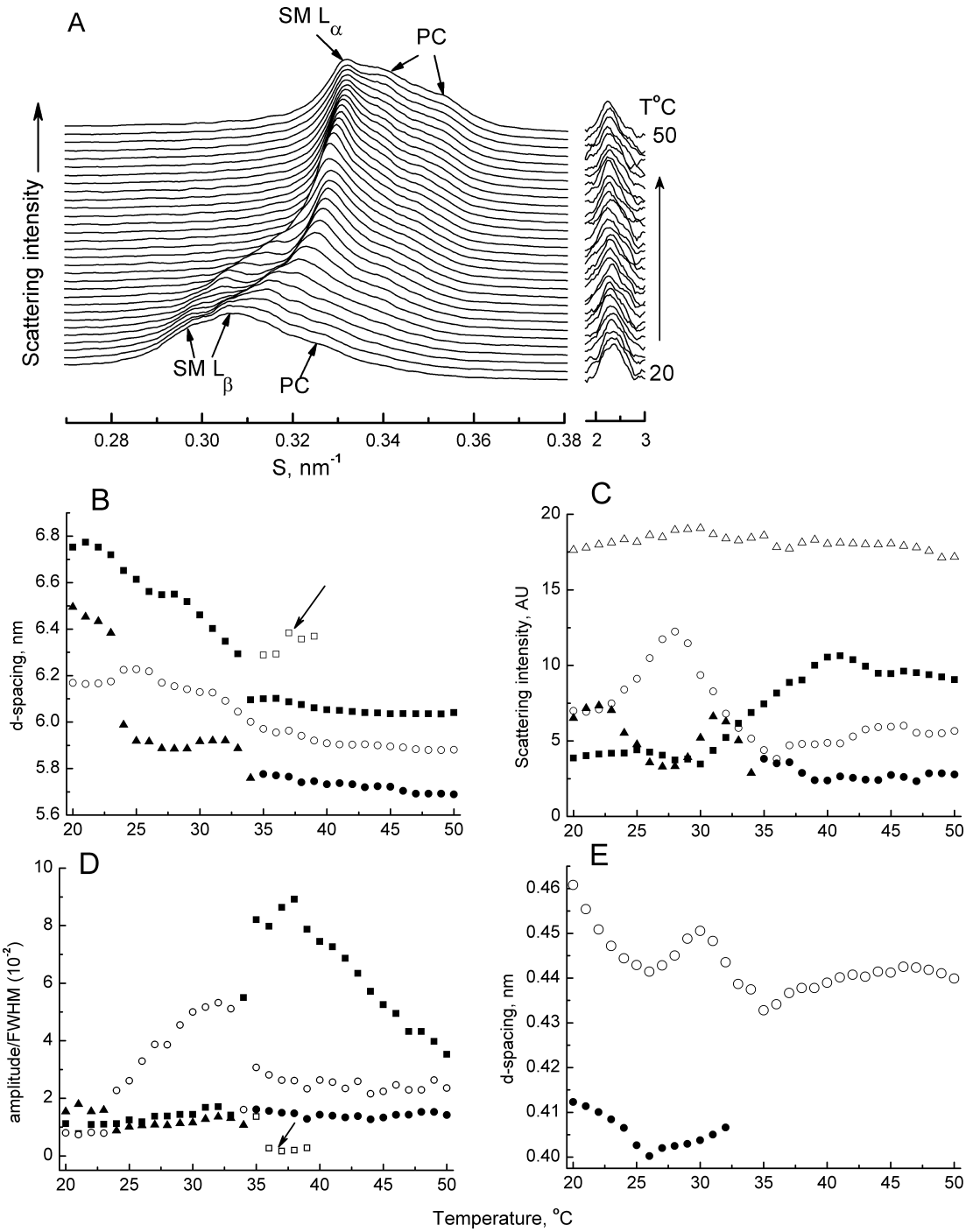

Figure 1. (A) Plot of SAXS intensity profiles in the region of second-order lamellar reflections from an aqueous dispersion of a binary mixture of egg-PC:egg-SM in equimolar proportions recorded at 1° intervals during a heating scan from 20 to 50 °C at 2 °C/min. Peaks are shown for gel-phase sphingomyelin (SM L_β), fluid-phase sphingomyelin (SM L_α), and fluid-phase phosphatidylcholine (PC). (B) Temperature-dependent changes, lamellar repeat spacings. (C) Scattering intensities. (D) Peak shape parameter. Peaks are assigned as egg-SM in gel (■,▲) and fluid (■) phases and egg-PC in fluid phase (○,●). The appearance of broad weak reflections at relatively high *d* spacings (□) in the region of the transition of the egg-SM from gel to fluid phase are indicated by arrows in the temperature range 35−39 °C. Criteria used for assignment of lamellar structures are given in the Supporting Information. (E) *d* spacings of peaks deconvolved from the corresponding WAXS intensity profiles.

the temperature dependence of *d* spacing provides supporting evidence that the diffraction originates from two independent lamellar structures. The relative scattering intensities from the two lamellar structures remains fairly constant up to the temperature of the onset of the phase transition of the egg-SM-enriched phase (Figure 2C). With increasing temperature there is a decrease in the scattering intensity from the egg-SM-enriched structure between 30 and 35 °C and a subsequent increase in scattering intensity at higher temperatures. In contrast to the progressive broadening of the egg-SM peak observed in the absence of cholesterol at temperatures above 40 °C, the egg-SM peak in the ternary mixture sharpens, indicating greater order in the lamellar structure (Figure 2D). The peak shape parameter, amplitude/fwhm, is correlated with the spatial distribution of the local director for the liquid-crystalline lamellar phase. The average packing of the hydrocarbon chains seen from the WAXS *d* spacing (Figure 2E) indicates that the chains become progressively disordered during the heating scan.

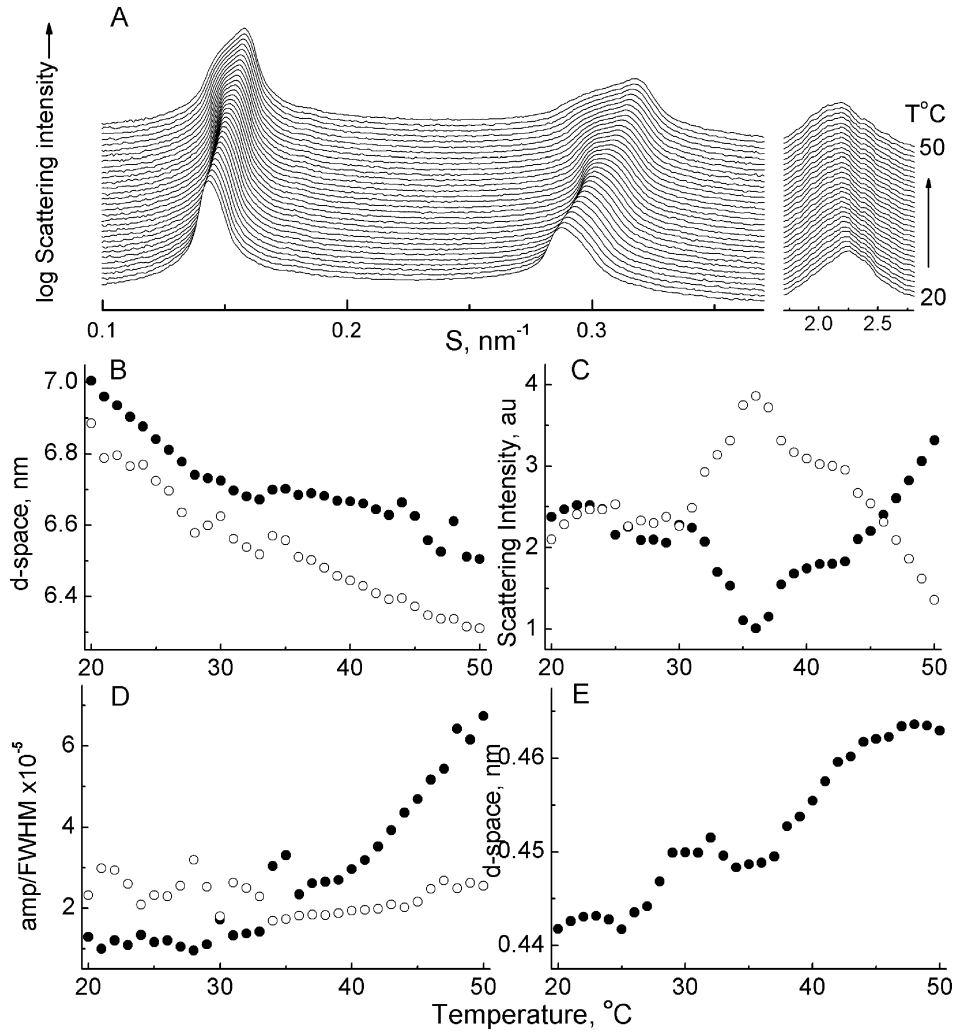

Figure 2. X-ray diffraction analysis of an aqueous dispersion of a ternary mixture of egg-PC:egg-SM:cholesterol in molar proportions 47.5:47.5:5 subjected to a heating scan from 20 to 50 °C at 2 °C/min. (A) X-ray scattering intensity profiles showing the first two orders of lamellar repeat spacings recorded at low angle (left) and intensity profiles recorded in the wide-angle region (right). (B) Relationship between temperature and lamellar *d* spacing. (C) Scattering intensity of the deconvolved second-order peaks. (D) Peak shape parameter indexed as amplitude/fwhm. Peak assignments are egg−SM-rich structure (●) and egg−PC-rich structure (○). (E) *d* spacing at maximum intensity in the WAXS region.

Analysis of the structure of an aqueous dispersion of a ternary mixture comprised of egg-PC:egg-SM:cholesterol in molar proportions 45:45:10 is presented in Figure 3. The patterns of temperature-dependent structural changes in diffraction peaks assigned as egg-PC and egg-SM-rich phases are similar to those observed with ternary mixtures containing 5 mol % cholesterol shown in Figure 2A. The lamellar *d* spacings of the egg-PC and egg-SM in the temperature range where the structure is in a more ordered configuration (<35 °C), however, are about 0.1 nm less in the ternary mixture containing 10 mol % cholesterol at corresponding temperatures (Figure 3B). The relative scattering intensities originating from the respective structures (Figure 3C) indicates that there is a decrease in the scattering originating from the egg-SM-rich structure and a corresponding increase from the egg-PC-rich structure up to about 35 °C, which is then reversed with increasing temperature. A progressive sharpening of the peak assigned as the egg-SM-rich phase indicating a greater order of the lamellar repeat structure is observed with increasing temperature above 35 °C (Figure 3D). As expected, the hydrocarbon chains become more disordered with increasing temperature (Figure 3E) and with a *d* spacing slightly greater than that observed in the ternary mixture containing 5 mol % cholesterol.

Increasing the proportion of cholesterol in the ternary mixture to 15 mol % results in similar temperature-dependent structural changes to those observed in mixtures containing 10 mol % cholesterol as can be seen from the summary data presented in Figure 4. An analysis of the SAXS/WAXS intensity profiles (Figure 4A) indicates that the lamellar *d* spacings of both structures (Figure 4B) are further reduced by about 0.1 nm at corresponding temperatures to that of the ternary mixture containing 10 mol % cholesterol. The temperature-dependent changes in scattering intensities originating from the two structures (Figure 4C) are similar to that seen with mixtures containing lower proportions of cholesterol. The bilayer order, as judged by sharpening of the peak assigned to the egg-PC-rich structure is markedly increased at temperatures below 35 °C (Figure 4D) but broadens at higher temperatures. As seen in mixtures with less cholesterol, the egg-SM-rich lamellar structure becomes more ordered with increasing temperatures above the main gel to fluid transition (T_m). No significant difference in temperature-dependent hydrocarbon chain order, however, can be distinguished between ternary mixtures containing 10 and 15 mol % cholesterol (Figure 3E cf. Figure 4E).

To assess the effect of the presence of cholesterol on the structure of bilayers of egg-PC and egg-SM at physiological

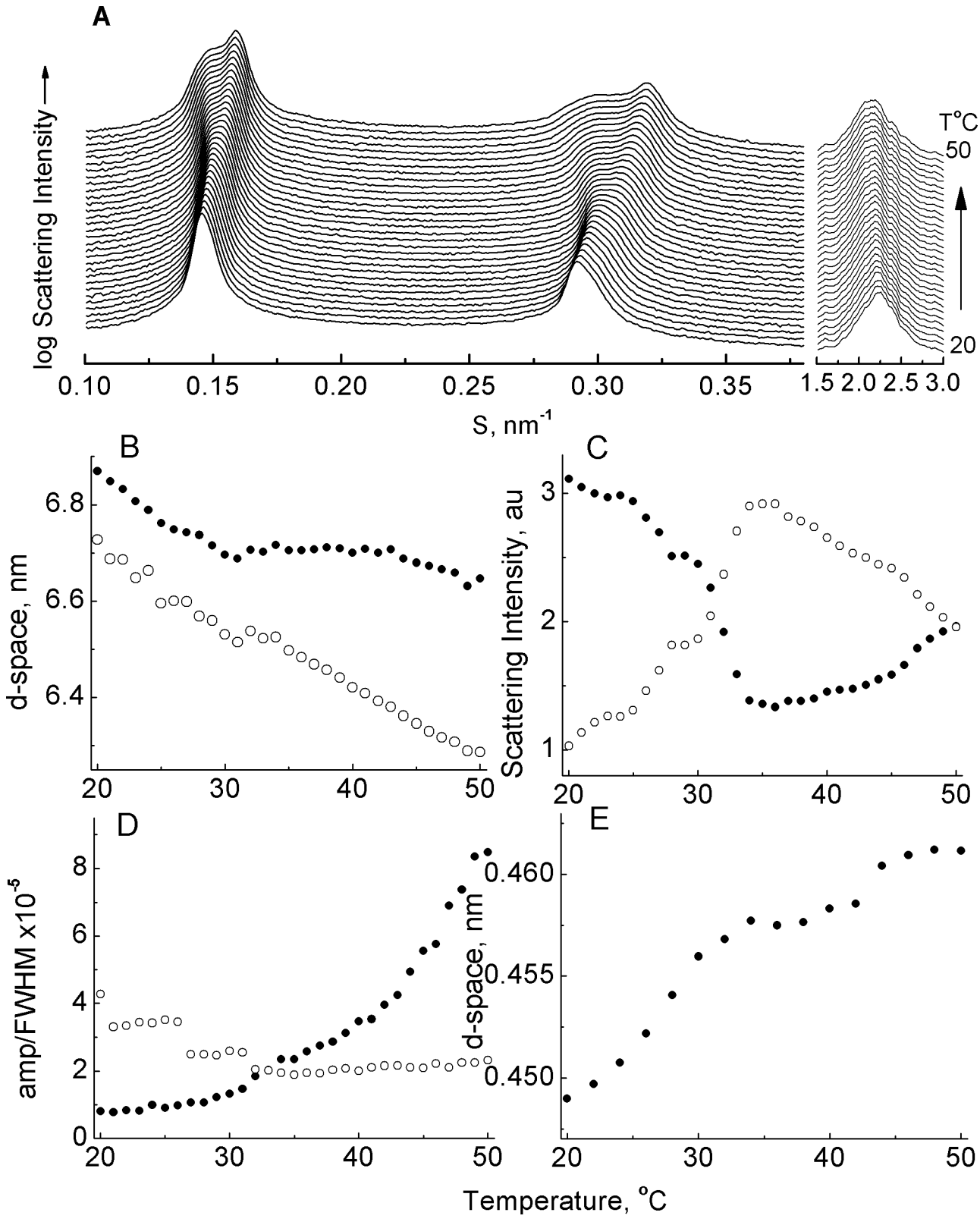

Figure 3. X-ray diffraction analysis of an aqueous dispersion of a ternary mixture of egg-PC:egg-SM:cholesterol in molar proportions 45:45:10 subjected to a heating scan from 20 to 50 °C at 2 °C/min. (A) X-ray scattering intensity profiles showing the first two orders of lamellar repeat spacings recorded at low-angle (left) and intensity profiles recorded in the wide-angle region (right). (B) Relationship between temperature and lamellar *d* spacing. (C) Scattering intensity of the deconvolved second-order peaks. (D) Peak shape parameter indexed as amplitude/fwhm. Peak assignments are as shown in Figure 2. (E) *d* spacing at maximum intensity in the WAXS region.

temperatures an analysis of the diffraction patterns recorded at 37 °C was undertaken, and the results are presented in Figure 5. Dispersions of pure egg-PC and egg-SM form lamellar structures that can each be deconvolved into two bilayer structures with different *d* spacings. As described above, an equimolar mixture of the two phospholipids can be resolved into at least two lamellar structures of *d* spacings that differ from those observed in the pure phospholipids. The fact that

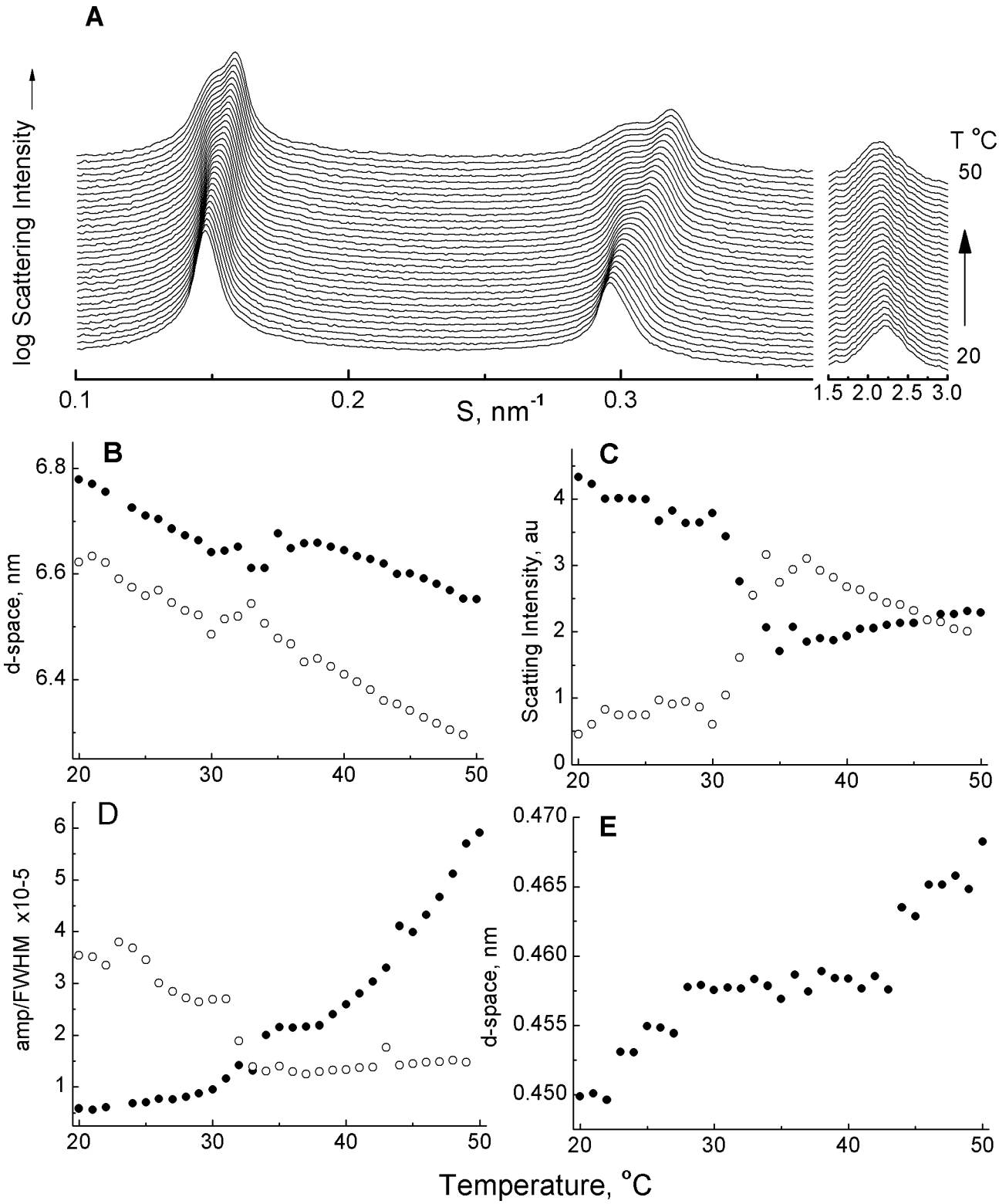

Figure 4. X-ray diffraction analysis of an aqueous dispersion of a ternary mixture of egg-PC:egg-SM:cholesterol in molar proportions 42.5:42.5:15 subjected to a heating scan from 20 to 50 °C at 2 °C/min. (A) X-ray scattering intensity profiles showing the first two orders of lamellar repeat spacings recorded at low-angle (left) and intensity profiles recorded in the wide-angle region (right). (B) Relationship between temperature and lamellar *d* spacing. (C) Scattering intensity of the deconvolved second-order peaks. (D) Peak shape parameter indexed as amplitude/fwhm. Peak assignments are as shown in Figure 2. (E) *d* spacing at maximum intensity in the WAXS region.

the *d* spacings of the phospholipids differ in the mixture is consistent with intimate mixing of small domains rather than large-scale separation of bilayers of pure lipids. Binary mixtures of equimolar proportions of egg-PC and cholesterol show a significant shift to greater *d* spacings compared to that of pure egg-PC. The effect of the presence of equimolar amounts of cholesterol in egg-SM cannot be compared directly with that of the pure egg-SM because this is partially in the gel phase at 37 °C in the absence of cholesterol, which significantly alters the structure of the bilayers. The lamellar reflections from dispersions containing increasing amounts of cholesterol in ternary mixtures comprised of equimolar proportions of egg-

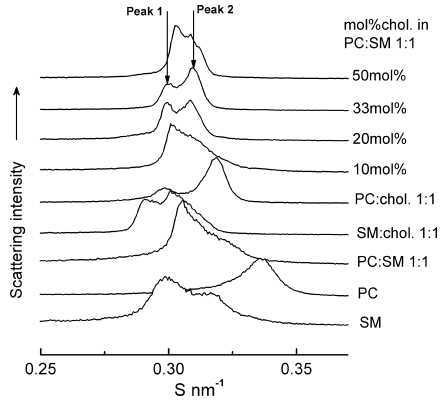

Figure 5. X-ray diffraction patterns in the region of the second-order lamellar reflections recorded at 37 °C from aqueous dispersions of composition shown on the right.

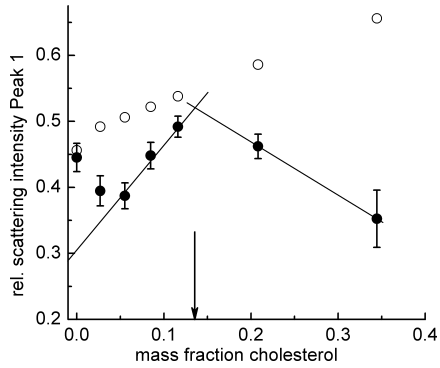

Figure 6. Relationship between mass fraction of cholesterol and relative scattering intensity of peak 1 identified in Figure 5 recorded from dispersions of equimolar mixtures of egg-PC and egg-SM containing varying molar fractions of cholesterol. Values represent mean ± SEM of combined first- and second-order reflections from 5 individual diffraction profiles (●). Calculated scattering intensity for the total mass of egg-SM + cholesterol in each ternary mixture (○). Arrow indicates the mass fraction of cholesterol forming a stoichiometric complex with egg-SM.

PC and egg-SM can be resolved into two peaks, the relative scattering intensities of which depend on the mol % cholesterol. Peak 1 is assigned on the basis of lamellar *d* spacing and electron spin resonance spectroscopy as liquid-ordered phase comprised of egg-SM and cholesterol and peak 2 as liquid-disordered phase of egg-PC and cholesterol.[15,16]

The scattering intensities from the egg-SM−cholesterol structure (peak 1) relative to the total scattering intensity of the Bragg peaks (peak 1 + peak 2) as a function of the mass fraction of cholesterol in the mixture is presented in Figure 6. Also shown in the figure is the contribution to the total scattering intensity due to egg-SM + cholesterol in each of the ternary mixtures. These values are calculated from the relative masses of the respective lipids in the ternary mixtures examined. In the absence of cholesterol the relative scattering intensity of peak 1 is 0.456. This compares with a value of 0.477 expected from all the egg-SM in the binary mixture. The observed value indicates that approximately 7 mol % of the egg-SM is mixed with egg-PC in the absence of cholesterol. The likely reason for this is that egg-SM contains about 6 mol % of molecular species with long (C-22, C-24) N-acyl fatty acids[17] and such sphingolipids mix with phospholipids to form a stoichiometric complex[34] and do not form coexisting bilayer phases in ternary mixtures with cholesterol and phosphatidylcholine that can be detected by pulsed field gradient NMR methods.[35]

The scattering intensity of peak 1 recorded from the ternary mixture containing 5 mol % cholesterol decreases to values less than expected if all the egg-SM remains in a separate phase, indicating that some egg-SM has partitioned into egg-PC. One possible explanation is that the presence of small amounts of cholesterol cause a disruption the intermolecular hydrogen-bond network between the egg-SM molecules that is responsible for their phase separation from the egg-PC. A linear regression function of the form $y = 0.017x + 0.297$ can be fitted to data obtained from ternary mixtures containing 10, 15, and 20 mol % cholesterol (mass fractions 0.055, 0.085, and 0.116, respectively). From the intercept of the regression line with the *y* axis it can be inferred that cholesterol at low concentrations induces mixing of 38% of the egg-SM with egg-PC. The relative intensity of peak 1 increases linearly in the range 10−20 mol % cholesterol, presumably because cholesterol forms structures with egg-SM by recruiting egg-SM molecules that have partitioned into the egg-PC-rich phase. The rate of this increase indicates that the ratio of sphingomyelin:cholesterol decreases with increasing proportions of cholesterol in the mixture. Because the *d* spacing of sphingomyelin coincides with that of peak 1 in mixtures containing between 10 and 20 mol % cholesterol it is not possible to determine how cholesterol is distributed within the structure. The relative intensity of peak 1 decreases in ternary mixtures containing proportions of cholesterol greater than about 20 mol % because cholesterol is in excess of the amount required to form a stoichiometric structure with all the egg-SM in the mixture. The excess cholesterol mixes with the egg-PC-rich phase. In the presence of cholesterol exceeding 33 mol %, different structures are formed as judged by a shift in lamellar *d* spacings of peak 1 to smaller values (see Figure 5) and there is a change in the relative scattering intensities of the deconvolved peaks. In mixtures containing more than about 50 mol % cholesterol the excess sterol forms crystals that are evidenced by a sharp Bragg peak at 3.4 nm and a number of characteristic peaks in the WAXS region.[36]

The stoichiometry of egg-SM and cholesterol in the structure comprising peak 1 can be obtained from the relative intensity of the peak at the intersection between the regression line fitted to mixtures containing 10−20 mol % cholesterol and the line passing through scattering intensities recorded from ternary mixtures containing 33 and 40 mol % cholesterol. The *x*-axis value indicates that the mass fraction of cholesterol in the ternary mixture is 0.13, giving proportions in the ternary mixture of egg-PC:egg-SM:cholesterol of approximately 38.5:38.5:22.5 expressed as mol %. Since the scattering in peak 1 accounts for 95% of the scattering due to egg-SM + cholesterol in the mixture, the stoichiometry of the complex is 1.7:1.

Discussion

Synchrotron X-ray powder diffraction provides a wealth of information about the structure of bilayer phases of complex lipid mixtures including bilayer dimensions and packing arrangements of the hydrocarbon chains.[37] A striking feature exhibited by mixed lipid bilayers is the extent to which they are coupled. This is manifest as the presence of discrete Bragg peaks that can be resolved by fits of Voigt functions despite differences in lamellar *d* spacings down to orders of 0.1 nm. Nevertheless, there is no information on the relative location of diffracting units so as to determine either the size of domains laterally within the bilayer planes or the extent of stacking of bilayers in multilamellar structures. Nevertheless, the respective order within the diffracting units can be assessed by the relative

widths of the Bragg peaks measured as peak amplitude/full width at half-maximum amplitude.

The conclusion that egg-SM and egg-PC are immiscible over the temperature range from 20 to 50 °C is supported by resolution of lamellar *d* spacings assigned to the individual phospholipids with intensities closely correlated with their proportions in the binary mixture (Figure 1D of the Supporting Information). The size of the laterally segregated domains is likely to be relatively small because the *d* spacings of the structures are much closer (differing by 0.25 nm) compared to the *d* spacings of the pure phospholipids, indicating an absence of large-scale phase separation. Similar conclusions have been reported from ^{2}H NMR studies of binary mixtures of ^{2}H-palmitoyl-SM and ^{2}H-palmitoyl-oleoyl-PC recorded at 40 °C.[38] The pure SM and PC have average order parameters of 0.221 and 0.144, respectively, which shift to intermediate positions (0.197 and 0.150) in an equimolar mixture. The quadrupolar splittings of the chain terminal methyl groups are within the error of the spectral measurement, indicating a rapid exchange between the two phospholipids takes place. In the presence of cholesterol, however, the quadrupolar splittings are increased to 1600 Hz, indicating that each phospholipid exists in its own distinctive environment. The size of these heterogeneous domains was estimated from the lifetime of one lipid species in its respective microdomain ($\tau \approx 0.1$ ms) and lipid diffusion constant ($D \approx 12$ pm^2 s^{-1}), giving a minimal diameter of the microdomains of about 140 nm. Assuming a surface area/phospholipid of 0.7 nm^2 the number of molecules in a coupled bilayer domain can be calculated as 40 000 lipid molecules. Calculations of the extended hydrocarbon chain lengths from the average order parameters yields a difference of 0.137 nm between SM and PC, which translates into a difference in bilayer thickness of the coupled structures of 0.28 nm. This is close to the difference in deconvolved Bragg *d* spacings in bilayer structures assigned to egg-SM (6.05 nm) and egg-PC (5.78 nm) in a binary mixture at 40 °C.

The factor responsible for lateral domain segregation between egg-SM and egg-PC in the fluid phase is likely due to intermolecular hydrogen bonds between sphingomyelin molecules. Intermolecular hydrogen bonds have been recorded in egg-SM in equimolar mixtures with egg-PC[12] or dipalmitoylphosphatidylcholine[39] by FTIR spectroscopy. Intermolecular hydrogen bonds have also been identified in molecular dynamic simulation studies of pure sphingomyelin[40] and mixtures of SM with PC and cholesterol.[41]

The present results show that addition of only 5 mol % of cholesterol to an equimolar mixture of egg-SM and egg-PC causes sphingomyelin molecules to mix with the egg-PC-rich phase, presumably by disrupting the intermolecular hydrogen-bond network. Cholesterol is estimated to be responsible for mixing of about 38% of the egg-SM molecules with the egg-PC-rich bilayers. In the presence of intermediate proportions of cholesterol (10−20 mol %) phase separation of an egg-SM−cholesterol structure is observed in which cholesterol progressively recruits sphingomyelin molecules from the egg-PC-rich bilayer. Cholesterol in proportions greater than about 20 mol % is in excess of the amount required to form the egg-SM−cholesterol structure, and this cholesterol partitions into the egg-PC-rich bilayers. The stoichiometry of egg-SM and cholesterol in the liquid-ordered structure equates to 37 mol % cholesterol.

There is much agreement between conclusions based on these X-ray diffraction measurements and those based on measurements of lateral diffusion of lipids using pulsed field gradient NMR methods.[42] Bilayers of equimolar proportions of dioleoylphosphatidylcholine and egg-SM show miscibility with cholesterol up to about 8 mol % cholesterol and separation into two phases in the presence of 10−37 mol % cholesterol. The domain sizes in these phase-separated regions was found to exceed 1 μm,[43] but replacement of the diunsaturated phospholipid with palmitoyloleoylphosphatidylcholine indicated that considerably smaller domains were formed in this case.[42] The suggestion that the driving force responsible for phase separation of liquid-ordered and liquid-disordered structure in ternary mixtures is the greater entropy required to incorporate disordered lipids into liquid-ordered structure is qualified by the present results. Thus, mixing of high T_m sphingomyelin with low T_m phosphatidylcholine is promoted by small amounts of cholesterol. Likewise, when proportions of cholesterol exceed 20 mol % there is a tendency for components of the liquid-ordered phase to mix with the fluid phospholipid phase.

Ternary Phase Diagram. Ternary phase diagrams said to model the creation of membrane rafts are comprised of mixtures of molecular species of phospholipids that phase separate into gel and fluid bilayers; cholesterol is believed to partition between the two phases with a coefficient that favors the phospholipid forming the gel phase. This model appears to be reliable for mixtures of glycerophospholipids[37] but not for mixtures of glycerophosphatidylcholines−sphingomyelins−cholesterol. The published ternary phase diagrams of these systems have been recently reviewed.[44] A variety of probe methods have been employed in constructing phase diagrams, and almost invariably they are performed at temperatures where the sphingomyelin is in the gel phase. Under these conditions gel- and fluid-phase separation of the two phospholipids is observed, and addition of increasing amounts of cholesterol up to about 30 mol % appears only to increase the size of the gel/liquid-ordered phase domains in the fluid phospholipid bilayer.[45] In such mixtures it is not easy to distinguish the gel phase of sphingomyelin from the liquid-ordered structure formed by sphingomyelin and cholesterol.

The present X-ray data recorded from binary and ternary mixtures of the lipids have been used to construct a phase diagram at 37 °C, and this is shown in Figure 7. Because the two phospholipids are extracts of biological tissue and comprised of a wide range of individual molecular species, Figure 7 is not strictly a ternary phase diagram. As such structures associated with the phase rules governing ternary phase diagrams may not apply. The most notable feature of the phase diagram of aqueous dispersions of egg-PC:egg-SM:cholesterol at 37 °C is that coexisting liquid-ordered and liquid-disordered (L_o + L_α) structures distinguished from the X-ray scattering intensity profiles dominate the phase diagram. The presence of the stoichiometric complex of egg-SM and cholesterol in all regions of the diagram appears to depend only on the sensitivity of the method used to detect it. Clearly, the SAXS/WAXS synchrotron X-ray diffraction method is relatively sensitive not only to define the structure in terms of characteristic lamellar and chain *d* spacings but also to assign the phase. Thus, liquid-ordered phase, as characterized by a wide-angle *d* spacing of about 0.44 nm, is only formed by interaction between egg-SM and cholesterol. Single-phase regions of liquid-disordered structure are comprised mainly of egg-PC and cholesterol, which does not form liquid-ordered phase at 37 °C.

Lamellar gel phase, as defined by a sharp wide-angle reflection at 0.41−0.42 nm, is not detected in any region of the phase diagram. The absence of gel phase has been noted in similar ternary mixtures at 37 °C.[29] This means that regions of

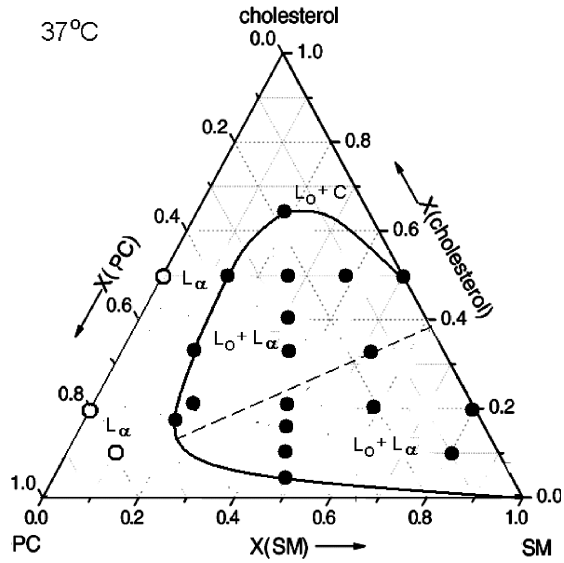

Figure 7. Ternary phase diagram of egg-PC:egg-SM:cholesterol at 37 °C. All compositions are expressed as mole fractions with respect to total phospholipid plus cholesterol: (●) two-phase composition $L_o + L_\alpha$; (○) single-component L_α structure; -------, egg-SM:cholesterol, 1.7:1 coexisting with bilayers of egg-PC.

three-phase coexistence, i.e., $L_o + L_\alpha + L_\beta$, are not observed in the phase diagram. The solubility limit of cholesterol in the phospholipid bilayers is manifest by a peak at about 3.4 nm in the SAXS region and characteristic sharp peaks in the WAXS region. The crystals of cholesterol coexist with bilayers of L_o phase when present in molar proportions greater than about 55 mol %.

A dashed line in the phase diagram shown in Figure 7 joins points of the two-phase coexistence of the diagram where the molar ratio of egg-SM:cholesterol is 1.7:1; this is the stoichiometry of the lipids in L_o bilayer structure. Below the line egg-SM is in excess of that required to form the stoichiometric complex with cholesterol and tends to partition into egg-PC bilayers. Above the line cholesterol is in excess and excluded from the complex and mixes with egg-PC. In this conception cholesterol does not partition between egg-SM-rich and egg-PC-rich phases as it does between mixtures of diacyl phosphatidylcholines with relatively high and low T_m, respectively.[37]

As already noted, it is not possible to distinguish pure sphingomyelin and the complex between sphingomyelin and cholesterol on the basis of lamellar *d* spacing to determine whether cholesterol is randomly distributed in the sphingomyelin-rich phase of ternary mixtures comprised of less that 22 mol % cholesterol. Evidence on this point has been reported from low-angle X-ray reflectivity experiments performed on monolayers of binary mixtures of egg-sphingomyelin and dihydrocholesterol at the air−water interface.[46] It was demonstrated that a stoichiometric complex of 1.86:1 of sphingomyelin:dihydrocholesterol coexists with uncomplexed sphingomyelin in binary mixtures up to proportions where all the sphingomyelin is complexed. Sterol molecules in excess of that required to form the stoichiometric complex are excluded and occupy a position in the film closer to the lipid−water interface than those forming the complex. In ternary lipid bilayers, however, excess sterol partitions into the egg-PC rich phase. More recent X-ray reflection studies of monolayers of binary mixtures of dipalmitoylphosphatidylcholine and cholesterol do not find evidence for formation of stoichiometric complexes even at physiological temperatures and surface pressures corresponding to that in bilayers.[47] This is consistent with the notion that the interaction between cholesterol and glycerophosphatidylcholines, on the one hand, and sphingomyelins, on the other, is fundamentally different. Because a lattice structure is likely to be required to provide the specificity needed to assemble cell membrane rafts the relevance of liquid-ordered phases formed between phosphatidylcholines and cholesterol to this process must be regarded with some circumspection.

Conclusion

Aqueous dispersions of binary mixtures of egg-SM and egg-PC form immiscible microdomains in bilayers at all temperatures between 20 and 50 °C. Addition of relatively small proportions of cholesterol disrupts the intermolecular hydrogen bonds between the sphingomyelin molecules, resulting in some mixing with the phosphatidylcholine. These sphingomyelin molecules are progressively recovered from the phosphatidylcholine phase with increasing proportions of cholesterol in formation of a stoichiometric complex of 1.7 sphingomyelins per cholesterol. Cholesterol in excess of that required to form the complex mixes with the phosphatidylcholine phase. The structure of the complex can be conceptualized as cholesterol surrounded by 7 hydrocarbon chains with each hydrocarbon chain in contact with, on average, 2 cholesterol molecules.

Acknowledgment. Thanks are given to Drs. Gunter Grossman and Jen Hiller for assistance in setting up beamlines 2.1 (Daresbury; grant 49098) and I22 (Diamond; grant sm764), respectively. Drs. G. Staneva and A. Dabkowska generously assisted with sample preparation and data collection. Dr. David Barlow provided helpful comments on data analysis.

Supporting Information Available: Criteria used to assign lamellar structures is detailed including methods used to deconvolute first- and second-order lamellar reflections from mixed dispersions of sphingomyelin and phosphatidylcholine and ternary mixtures with cholesterol; Assignments were made on the basis of (1) lamellar *d* spacings compared with bilayer dispersions of the pure lipids, (2) changes in scattering intensity of peaks correlated with the proportion of particular lipids in the mixture, (3) temperature-dependent profiles of Bragg peaks in small and wide-angle scattering regions. This material is available free of charge via the Internet at http://pubs.acs.org.

References and Notes

(1) Suzuki, K. G. N.; Fujiwara, T. K.; Edidin, M.; Kusumi, A. *J. Cell Biol.* **2007**, *177*, 731.
(2) Simons, K.; Toomre, D. *Nat. Rev. Mol. Cell Biol.* **2000**, *1*, 31.
(3) Edidin, M. *Ann. Rev. Biophys. Biomol. Struct.* **2003**, *32*, 257.
(4) Tolar, P.; Sohn, H. W.; Liu, W. L.; Pierce, S. K. *Immunol. Rev.* **2009**, *232*, 34.
(5) Lindner, R.; Naim, H. Y. *Exp. Cell Res.* **2009**, *315*, 2871.
(6) Feigenson, G. W. *Biochim. Biophys. Acta: Biomembr.* **2009**, *1788*, 47.
(7) Goni, F. M.; Alonso, A.; Bagatolli, L. A.; Brown, R. E.; Marsh, D.; Prieto, M.; Thewalt, J. L. *Biochim. Biophys. Acta: Mol. Cell Biol. Lipids* **2008**, *1781*, 665.
(8) Rog, T.; Pasenkiewicz-Gierula, M.; Vattulainen, I.; Karttunen, M. *Biochim. Biophys. Acta: Biomembr.* **2009**, *1788*, 97.
(9) Ahmed, S. N.; Brown, D. A.; London, E. *Biochemistry* **1997**, *36*, 10944.
(10) Brown, R. E. *J. Cell Sci.* **1998**, *111*, 1.
(11) London, E.; Brown, D. A. *Biochim. Biophys. Acta: Biomembr.* **2000**, *1508*, 182.
(12) Veiga, M. P.; Arrondo, J. L. R.; Goni, F. M.; Alonso, A.; Marsh, D. *Biochemistry* **2001**, *40*, 2614.
(13) Xu, X. L.; Bittman, R.; Duportail, G.; Heissler, D.; Vilcheze, C.; London, E. *J. Biol. Chem.* **2001**, *276*, 33540.
(14) Epand, R. M. *Biochim. Biophys. Acta: Biomembr.* **2008**, *1778*, 1576.
(15) Chachaty, C.; Rainteau, D.; Tessier, C.; Quinn, P. J.; Wolf, C. *Biophys. J.* **2005**, *88*, 4032.

(16) Tessier, C.; Staneva, G.; Trugnan, G.; Wolf, C.; Nuss, P. *Colloids Surfaces B: Biointerfaces* **2009**, *74*, 293.
(17) Quinn, P. J.; Wolf, C. *Biochim. Biophys. Acta: Biomembr.* **2009**, *1788*, 1877.
(18) Ipsen, J. H.; Karlstrom, G.; Mouritsen, O. G.; Wennerstrom, H.; Zuckermann, M. J. *Biochim. Biophys. Acta* **1987**, *905*, 162.
(19) Ipsen, J. H.; Mouritsen, O. G.; Zuckermann, M. J. *Biophys. J.* **1989**, *56*, 661.
(20) de Almeida, R. F. M.; Fedorov, A.; Prieto, M. *Biophys. J.* **2003**, *85*, 2406.
(21) de Almeida, R. F. M.; Loura, L. M. S.; Fedorov, A.; Prieto, M. *J. Mol. Biol.* **2005**, *346*, 1109.
(22) Mateo, C. R.; Acuna, A. U.; Brochon, J. C. *Biophys. J.* **1995**, *68*, 978.
(23) Pokorny, A.; Yandek, L. E.; Elegbede, A. I.; Hinderliter, A.; Almeida, P. F. F. *Biophys. J.* **2006**, *91*, 2184.
(24) Veatch, S. L.; Keller, S. L. *Phys. Rev. Lett.* **2005**, *94*, 148101.
(25) Henriksen, J.; Rowat, A. C.; Brief, E.; Hsueh, Y. W.; Thewalt, J. L.; Zuckermann, M. J.; Ipsen, J. H. *Biophys. J.* **2006**, *90*, 1639.
(26) Mannock, D. A.; Lewis, R. N. A. H.; McMullen, T. P. W.; McElhaney, R. N. *Chem. Phys. Lipids* **2010**, *163*, 403.
(27) Quinn, P. J.; Wolf, C. *Biochim. Biophys. Acta: Biomembr.* **2009**, *1788*, 1126.
(28) Maulik, P. R.; Shipley, G. G. *Biochemistry* **1996**, *35*, 8025.
(29) Staneva, G.; Chachaty, C.; Wolf, C.; Koumanov, K.; Quinn, P. J. *Biochim. Biophys. Acta: Biomembr.* **2008**, *1778*, 2727.
(30) Addink, E. J.; Beintema, J. *Polymer* **1961**, *2*, 185.
(31) Zhang, R. T.; Suter, R. M.; Nagle, J. F. *Phys. Rev. E* **1994**, *50*, 5047.
(32) Yao, T.; Jinno, H. *Acta Crystallogr., Sect. A* **1982**, *38*, 287.
(33) Chemin, C.; Bourgaux, C.; Pean, J. M.; Pabst, G.; Wuthrich, P.; Couvreur, P.; Ollivon, M. *Chem. Phys. Lipids* **2008**, *153*, 119.
(34) Quinn, P. J. *Biochim. Biophys. Acta: Biomembr.* **2009**, *1788*, 2267.
(35) Filippov, A.; Oradd, G.; Lindblom, G. *Biophys. J.* **2006**, *90*, 2086.
(36) Self-Medlin, Y.; Byun, J.; Jacob, R. F.; Mizuno, Y.; Mason, R. P. *Biochim. Biophys. Acta: Biomembr.* **2009**, *1788*, 1398.
(37) Chen, L.; Yu, Z. W.; Quinn, P. J. *Biochim. Biophys. Acta: Biomembr.* **2007**, *1768*, 2873.
(38) Bunge, A.; Muller, P.; Stockl, M.; Herrmann, A.; Huster, D. *Biophys. J.* **2008**, *94*, 2680.
(39) Villalain, J.; Ortiz, A.; Gomez Fernandez, J. C. *Biochim. Biophys. Acta* **1988**, *941*, 55.
(40) Mombelli, E.; Morris, R.; Taylor, W.; Fraternali, F. *Biophys. J.* **2003**, *84*, 1507.
(41) Pandit, S. A.; Jakobsson, E.; Scott, H. L. *Biophys. J.* **2004**, *87*, 3312.
(42) Lindblom, G.; Oradd, G. *Biochim. Biophys. Acta: Biomembr.* **2009**, *1788*, 234.
(43) Filippov, A.; Oradd, G.; Lindblom, G. *Biophys. J.* **2004**, *86*, 891.
(44) Marsh, D. *Biochim. Biophys. Acta: Biomembr.* **2009**, *1788*, 2114.
(45) Sullan, R. M. A.; Li, J. K.; Hao, C.; Walker, G. C.; Zou, S. *Biophys. J.* **2010**, *99*, 507.
(46) Ratajczak, M. K.; Chi, E. Y.; Frey, S. L.; Cao, K. D.; Luther, L. M.; Lee, Y. C.; Majewski, J.; Kjar, K. *Phys. Rev. Lett.* **2009**, *103*, 028103.
(47) Ivankin, A.; Kuzmenko, I.; Gidalevitz, D. *Phys. Rev. Lett.* **2010**, *104*, 108101.

JP107490A